

## ABSTRACT

Title of Document: SPATIAL PATTERNS AND POTENTIAL  
MECHANISMS OF LAND DEGRADATION  
IN THE SAHEL

Khaldoun Rishmawi, Doctor of Philosophy,  
2013

Directed By: Professor Stephen D. Prince  
Department of Geography

There is a great deal of debate on the extent, causes and even the reality of land degradation in the Sahel. On one hand, extrapolations from field-scale studies suggest widespread and serious reductions in biological productivity threatening the livelihoods of many communities. On the other hand, coarse resolution remote sensing studies consistently reveal a net increase in vegetation production exceeding that expected from the recovery of rainfall following the extreme droughts of the 1970s and 1980s, thus challenging the notion of widespread, subcontinental-scale degradation. Yet, the spatial variations in the rates of vegetation recovery are not fully explained by rainfall trends which suggest additional causative factors. In this dissertation, it is hypothesized that in addition to rainfall other climatic variables and anthropogenic uses of the land have had measurable impacts on vegetation production. It was found that over most of the Sahel, the interannual variability in

itqykpi"ugcuqp" PFXK" \*wugf" cu" c" rtqz{ "qh" xgigvation productivity) was strongly related to rainfall, humidity and temperature while the relationship with rainfall alone was generally weaker. The climate- PFXK" tgnvkkpujkru were used to predict rvgpvkcn" PFXK="vjcv"ku"vjg" PFXK"gzrgevfgf"kp"tgurqpug"vo climate variability alone excluding any human-induced changes in productivity. The differences between rtgfkevgf"cpf"qdugtvgf" PFXK" ygtg"tgi tguugf" cickpuv"vkog"vq" fgvgev" cp{"nqpi"vgt o" (positive or negative) trends in vegetation productivity.

It was found that over most of the Sahel the trends either exceeded or did not significantly depart from what is expected from the trends in climate. However, substantial and spatially contiguous areas (~8% of the total area of the Sahel) were characterized by significant negative trends. To test whether the negative trends were in fact human-induced, they were compared with the available data on population density, land use pressures and land biophysical properties that determine the susceptibility of land to degradation. It was found that the spatial variations in the trends of the residuals were not only well explained by the multiplicity of land use pressures but also by the geography of soil properties and percentage tree cover.

SPATIAL PATTERNS AND POTENTIAL MECHANISMS OF LAND  
DEGRADATION IN THE SAHEL

By

Khaldoun Rishmawi

Dissertation submitted to the Faculty of the Graduate School of the  
University of Maryland, College Park, in partial fulfillment  
of the requirements for the degree of  
Doctor of Philosophy  
2013

Advisory Committee:  
Professor Stephen Prince, Chair  
Professor Eric Kasischke  
Professor Ralph Dubayah  
Professor James Kellner  
Professor Rachel Pinker

© Copyright by  
Khaloun Rishmawi  
2013

*To my wife,*

*O q p k e c " í*

## Acknowledgements

I would like to thank the Fulbright Scholarship Program and the United States Department of State's Bureau of Educational and Cultural Affairs (ECA) for sponsoring the first two years of my PhD program. Additional funding was provided by the NASA ROSES program grant NASA.NNX08AL56G awarded to Professor Stephen Prince (PI).

I would like to thank Professor Yongkang Xue (Department of Geography, University of California - Los Angeles) for his guidance on the application of the Simplified Simple Biosphere (SSiB) model and I deeply appreciate the support provided by my friend and colleague Dr. Jyoteshwar Nagol who provided guidance and tools for the processing of the Satellite data.

I am particularly grateful to my advisor, Professor Stephen Prince, for his mentorship and support during the course of my PhD studies. His knowledge, enthusiasm and dedication provided an unmatched learning experience.

## Table of Contents

Acknowledgements .....	iii
Table of Contents .....	iv
List of Tables .....	vi
List of Figures .....	vii
Chapter 1: Introduction .....	1
1.1 Background .....	1
1.2 Study area.....	3
1.3 The controversy surrounding land degradation in the Sahel .....	6
1.4 Temporal scales for the detection of land degradation .....	11
1.5 Remote sensing of vegetation production.....	12
1.6 Monitoring land degradation with satellite remotely sensed data .....	14
1.7 Research Objectives.....	18
1.8 Outline of Dissertation.....	19
Chapter 2: Vegetation responses to climate variability .....	21
2.1 Introduction.....	21
2.2 Material and Methods .....	24
2.2.1 Remote sensing data .....	24
2.2.2 Meteorological data .....	26
2.2.3 Estimating phenological transition dates and the length of the growing season .....	26
40406" Tgncvkqpujkr"qh"cppwcn" PFXK" ykvj"cppwcn"vqvcn"rtgekrkvcvkqp .....	27
40407" Tgncvkqpujkr"qh"itqykpi"ugcuqp" PFXK" ykvj"kpvtcugcuqpcn"rtgekrkvcvkqp" distribution .....	28
40408" Tgncvkqpujkr"qh"itqykpi"ugcuqp" PFXK" ykvj"kpvtcugcuqpcn"rtgekrkvcvkqp" distribution .....	29
2.2.6 Soil-vegetation-atmosphere transfer modeling .....	30
2.3 Results.....	34
2.3.1 Phenological transition dates .....	34
2.3.2 Relationship of NDVI with rainfall .....	36
40505" Tgncvkqpujkr"qh"itqykpi"ugcuqp" PFXK" ykvj"kpvtcugcuqpcn"rtgekrkvcvkqp" distribution .....	38
40506" Tgncvkqpujkr"qh"itqykpi"ugcuqp" PFXK" ykvj"jwokfv{"cpf"vgorgtcwvtg .	40
2.3.5 Soil-vegetation-atmosphere transfer modeling .....	44
2.4 Discussion.....	53
2.4.1 Phenological transition dates .....	53
40604" Tgncvkqpujkr"qh" PFXK" ykvj"enkocvg"xctkcdknkv{ .....	54
2.5 Conclusions.....	59

Chapter 3: Long term trends in vegetation productivity .....	62
3.1 Introduction.....	62
3.2 Material and methods.....	66
3.2.1 Remote sensing data .....	66
3.2.2 Meteorological data .....	68
3.2.3 Residual trends.....	69
3.3 Results.....	71
3.3.1 Residual trends.....	71
3.3.2 Residual trends.....	75
3.4 Discussion .....	78
3.5 Conclusions.....	84
 Chapter 4: Are changes in productivity related to demographic pressures?.....	85
4.1 Introduction.....	85
4.2 Material and methods.....	88
4.2.1 Demographic and land use pressures data .....	88
4.2.2 Soil and land cover data.....	90
4.2.3 Relating residual trends to demographic pressures, land cover, and soil variables .....	92
4.3 Results.....	94
4.4 Discussion.....	106
4.5 Conclusions.....	107
 Chapter 5: Synthesis, discussion and significance.....	110
5.1 Context.....	110
5.2 Findings.....	111
5.3 Relevance to climate studies, global carbon budget and food security .....	116
5.4 Monitoring versus mapping land degradation .....	120
5.5 Future research.....	122
 Appendix 1: Reconstruction of daily AVHRR NDVI data .....	127
A1.1 Background .....	127
A1.2 LTDR AVHRR data.....	128
A1.3 LTDR AVHRR data processing .....	129
A1.4 LTDR AVHRR data relative errors .....	134
 Appendix 2: Comparison between residual trend results and field observations ....	140
 Bibliography .....	146



## List of Tables

Table 2.1 Information on sites used for sensitivity studies. GUMA: the period of Greenup to maturity. MASE: the period of Maturity to senescence.....	33
95% confidence level are the averages of all regression equations estimated for each 9 pixel arrangement of adjacent pixels.....	72
Table 3.2 Percentage land area with significant negative and positive trends in precipitation, SHUM specific humidity, temperature. OLS ordinary least squares and upper quartile regression.....	77
Table 4.1 Correlation values (r) between residual trends and demographic and land use pressures. The multivariate correlation value was estimated from the relation of residual trend values to %HANPP, LSU/NPP, and %crop cover/mean annual precipitation. OLS ordinary least squares and upper quartile regression.....	96
Table 4.2 Spatial variation in residual trend values explained by land use (livestock density and cropping density), land use and soil properties, and land use and land cover using RF regression tree models. LSU/NPP stock unit density normalized by site primary productivity, CD/MAR Cropping density normalized by Mean Annual Precipitation.....	99
Table 4.3 Spatial variation in residual trend values explained by %HANPP and soil properties, %HANPP and vegetation cover, %HANPP and fire density, and %HANPP soil bulk density fraction tree cover using RF regression tree models.....	100
Table A2.1 Comparisons between residual trend results and published literature on the status of land degradation and land use pressure in the Sahel. Table continues on next page.	140

## List of Figures

Figure 1.1 Dryland systems of the study area and the extent of the Sahel.....	4
Figure 1.2 Wet season (June through October) Sahel precipitation anomalies (1980-2006) (1980 are from the National Oceanic and Atmospheric Administration (NOAA) National Climatic Data Center (NCDC).....	6
Figure 2.1 Scatter plot of MODIS and AVHRR phenological transition dates of 250 randomly selected sites. The plot shows the relationship between the dates of onset of greenness increase (RMSE = 15.5 days, $r=0.89$ ). Crosses (+) represent the dates of onset of maturity (RMSE = 29 days, $r = 0.2$ ). The plot also shows the dates of onset of dormancy (RMSE = 29 days, $r = 0.2$ ).....	35
Figure 2.2 Spatial variation in averaged values (1982-2006) of the dates of onset of greenness increase (days). The map in (d) is the between years variation ( $\pm 2$ standard deviations) in the onset date of greenness increase. The abbreviation DOY is the Julian day of the year.....	36
Figure 2.3 Coefficients of determination ( $r^2$ ) for (a) annual rainfall (V) and (b) 1100mm rainfall isohyet.....	37
Figure 2.4 Percentage area with significant rainfall relationships (bars) in each rainfall range and the spatial average of the coefficient of determination ( $r^2$ ) (points) of all pixels within each rainfall range.....	38
Figure 2.5 Spatial distributions of (a) the coefficients of determination (adjusted multiple $R^2$ ) and (b) the change in the percentage of variance explained by the addition of additional variables over the 300mm, 700mm and 1100mm rainfall isohyet.....	39
Figure 2.6 Coefficients of (a) seasonal rainfall variance, and (b) seasonal rainfall skewness obtained from precipitation variance and skewness. Missing values (white pixels) are areas with multicollinearity between explanatory variables, or where the coefficients were insignificantly different from zero ( $p>0.05$ ). The dashed lines from north to south are the 300mm, 700mm and 1100mm rainfall isohyet.....	40
Figure 2.8 Regression coefficients of (a) specific humidity, and (b) air temperature obtained from precipitation variance and skewness. Missing values (white pixels) are areas with high multicollinearity between explanatory variables, or where the coefficients were insignificantly different from zero ( $p>0.05$ ). The dashed lines from north to south are the 300mm, 700mm and 1100mm rainfall isohyet.....	42
Figure 2.9 A randomly drawn sample (10%) representing the relationship of rainfall climatology to (a) specific humidity ( $\text{kg}_m/\text{kg}_{\text{Air}}^{-1}$ ) and (b) specific humidity coefficient.....	43
Figure 2.10 Mean absolute values of the standardized coefficients of the multivariate regression between NDVI and explanatory variables (precipitation, specific humidity and temperature) summarized for the land cover types. Error bars are $\pm 1$ standard deviation around the mean.....	44
Figure 2.11 The response of daily soil moisture at root depth to changes in precipitation, temperature, and specific humidity averaged for the period from greenup to maturity (greenup period, grey diamonds; left hand axis) and from maturity to senescence (maturity period, black circles; right hand axis). Note the different ranges on the y-axis between the two periods.....	47

Figure 2.12	The response of stomatal resistance to changes in precipitation, temperature, and specific humidity averaged for the period from greenup to maturity (greenup period, grey diamonds; left hand axis) and from maturity to senescence (maturity period, black circles; right hand axis). Note the different ranges on the y axis between sites. Figure continues on next page.....	49
Fig. 2.13	The response of Net primary productivity to changes in precipitation, temperature, and specific humidity averaged for the period from greenup to maturity (greenup period, grey diamonds; left hand axis) and from maturity to senescence (maturity period, black circles; right hand axis). Note the different ranges on the y axis between sites. Figure continues on next page.....	51
7	h	
	their prediction intervals at the 95% confidence level for a crop (S.725W, 1.525N)	
	difference between the OLS and UQ precipitation coefficient values for all sites throughout the Sahel. (c) The ability of precipitation (model A), precipitation, specific humidity and temperature (model C) and precipitation and its seasonal distribution (model B) to	73
7	Vh prediction errors: (a) prediction errors of the OLS regression between	
	speci	
	distribution variance and skewness (model C). (d) Frequency distribution of NDVI for the three models normalized by the range of NDVI values [PE/(maximum NDVI minimum NDVI)], and (e) frequency distribution of the values in (b) and (c)...	74
Figure 3.3	(a) Trends (slopes) of NDVI residuals (observed potential) regressed over time at four locations in the Sahel. The trends in (a) and (b) are significantly different from zero (p value of the F test < 0.05 and their absolute values are greater than their respective), whereas the trends in (c) and (d) are not significant on the basis of the same criteria. Bars are residual errors at the 95% confidence level.....	76
Figure 3.4	(a) Trends (slopes) of NDVI residuals (observed potential) over time as obtained from the six residual trend models (A through F; see table.1).....	78
Figure 4.1	a: Trends (slopes) of NDVI residuals (observed potential) over time as obtained from the OLS regression of NDVI with precipitation, specific humidity and temperature (see table 4.1). b d: datasets used to explore the relationship between residual trends and land use pressures (Ramankutty et al 2008, FAO 2011).....	91
Figure 4.2	Mean residual trend values (observed potential) within groupings of (a) population density (person/ha); (b) percentage human appropriation of NPP; (c) livestock unit density (unit/ha); (d) livestock unit density normalized by site productivity; (e) fraction land area used for crops; and (f) fraction land area used for crops normalized by mean annual precipitation. Filled circles are trends of the residuals where potential NDVI was obtained from OLS multivariate regression between NDVI and precipitation, specific humidity, and temperature. Open circles are trends of the residuals where potential NDVI was obtained from OLS multivariate regression between NDVI and precipitation, its seasonal variance and skewness. Error bars are $\pm 1$ standard deviation around the mean.....	97
Figure 4.3	The upper panel demonstrates the relationship between significant residual four explanatory variables, namely, soil erodibility factor, livestock unit density normalized by site productivity (LSU/NPP), fraction land used for agriculture (cropping density), and population density: (a) is a biplot of the of the first two principal component loadings of a principal component analysis, and (b) are variable importance values calculated by the regression tree model Random Forest. The lower panel demonstrates the ability of the four explanatory variables to explain variation in residual trend values: (c) is a comparison	

between residual trend values modeled from the NDVI data time series and residual trend values predicted by RF analysis) and (d) is a histogram of the differences between the plotted values in (c). Residual trends insignificantly different from zero were excluded from the analysis..... 101

Figure 4.4 The upper panel demonstrates the relationship between significant trends and the three explanatory variables, namely, fraction tree cover (fTree), percentage human appropriation of NPP (%HANPP), and soil bulk density: (a) is a biplot of the of the first and second principal component loadings of a principal component analysis and (b) are variable importance values calculated by the regression tree model Random Forest(RF). The lower panel demonstrates the ability of the three explanatory variables to explain the variation in residual trend values: (c) is a comparison between residual trend values modeled from the NDVI data time series (x-axis) and residual trend values predicted by RF analysis (y-axis) and (d) is a histogram of the differences between the plotted values in (c). Residual trends insignificantly different from zero were excluded from the analysis..... 102

Figure 4.5 Pruned regression tree showing the hierarchical relations of residual trends to land use, demographic pressures and soil erosion. Regression tree  $r^2=0.6$  and RMSE = 0.23. 104

Figure 4.6 Pruned regression tree showing the hierarchical relations of residual trends to %HANPP and to soil and land cover properties. Regression  $r^2=0.65$  and RMSE = 0.21..... 105

Figure A1.1 Reference NDVI and their corresponding predicted values for the linear (black diamonds), quadratic (grey diamonds) and upper quadratic (open circles) regression models for a savanna site. For clarity 2 randomly selected reference samples out of 200 are shown. The piecewise quadratic regression model had the lowest MBE, RMSEs, and RMSEu. .... 134

Figure A1.2 Area averaged mean bias error (MBE), systematic root mean squared error (RMSEs) and random root mean squared error (RMSEu) in NDVI units for the most widespread land cover types in the Sahel. Error bars are one standard deviation around the mean..... 136

Figure A1.3 Map showing the spatial variation of RMSEu values for LTDR AVHRR NDVI data. Water bodies, deserts, wetlands, urban areas, and locations with no paired AVHRR MODIS data points were excluded (black areas)..... 136

Figure A1.4 Mean RMSE values summarized for land cover types in the Sahel for interpolations using linear, upper quantile and quadratic regression models. Error bars are  $\pm 1$  standard deviation of the RMSE values and represent the spatial heterogeneity of RMSE values within each land cover type..... 138

Figure A1.5 The series of AVHRR NDVI data for a grassland vegetation at 27.725°E, 12.375°N, corrected for: 1) BRDF (black dots), 2) cloud cover (crosses), and 3) missing values (grey circles). Error bars are NDVI values  $\pm 1$  RMSE..... 139

# E j c r v k p v b e f w e v k q p

## 1.1 Background

Drylands encompass all lands where the climate is classified as arid, semi-arid and dry sub-humid<sup>1</sup> (UNEP 1992; UNEP 1997; Adeel *et al.* 2005). Global drylands are home to approximately 4 billion people (UNEP 2006) and contain approximately 62% of the world's population (Safriel *et al.* 2005; Safriel 2007a) with a total carbon pool of approximately 1420 gigatons (Gt) that is almost twice the size of the atmospheric pool (Lal 2004). Land degradation is considered as one of the major environmental problems in drylands (UNCED 1992; UNCCD 1994; Reynolds *et al.* 2007a). The livelihoods of some 250 million people are believed to be directly affected, a figure that is likely to increase substantially in the face of population growth and climate change (Reynolds *et al.* 2007b). In addition to its threat to human well-being, land degradation reduces carbon sequestration and organic soil carbon deposition (Falkowski *et al.* 2000; Prince 2002), disrupts the surface water balance (Balling *et al.* 1998; Taylor *et al.* 2002), increases atmospheric dust concentration (Prospero & Lamb 2003), reduces biodiversity (Maestre *et al.* 2012), and may intensify and prolong drought episodes through vegetation-climate feedbacks (Charney 1975; Clark *et al.* 2001; Taylor *et al.* 2002; Giannini *et al.* 2003).

Various authors have provided useful compendiums (Mainguet 1991; Thomas & Middleton 1994; Reynolds 2001). It is generally agreed that land degradation implies long-term

---

<sup>1</sup> Arid ( $0.05 \times \text{Precipitation(P) / Potential evapotranspiration (PET)} > 2042.097$  in  $\text{days/yr}$ ), semi-arid ( $0.05 \times \text{Precipitation(P) / Potential evapotranspiration (PET)} > 2072.970$  in  $\text{days/yr}$ ), and dry sub-humid ( $0.05 \times \text{Precipitation(P) / Potential evapotranspiration (PET)} > 2087.3420$  in  $\text{days/yr}$ ).

reductions in the biological productivity of the land resulting from one or a combination of processes including reductions in vegetation productivity and cover, uqkn" fg itcfvckqp" cpf" ejcpi gu" kp" urgek gu" eq o rqukvkqp0" " Vjg" vgt o" õncpfö" jcu" dggp" defined by the United Nations Convention to Combat Desertification (UNCCD) as õvjg"vgttguvtkcn"dkq-productive system that comprises soil, vegetation, other biota, and vjg"geqnqikecn"cpf" j {ftqnqikecn" rtqeguugu"vjcv" qrgtcvg" ykvj kp"vjg"u{uvgoö" (UNCCD 1994).

Despite its acknowledged importance, the nature and causes of land degradation have remained stubbornly intractable (Thomas & Middleton 1994; Reynolds *et al.* 2002; Nicholson 2011a). This has been more evident in the Sahel region of Africa than in any other part of the world where divergent assessments have led to more disagreement and controversy than consensus (Helldén 1991; Nicholson *et al.* 1998). Much of the controversy, it is generally agreed, have resulted from wpycttcpvgf"gzvtrqncvkqpu"htqo" nk okvgf" fcv" qt" uwdlgevkg" õgzrgtvö" qrkpkqpu."htqo" the lack of a consensus definition, and from the confusion between climate-induced short-term ecosystem dynamics (e.g. short-term response to periodic droughts) and land degradation -(a long-term response resulting from chronic and severe disturbances) - (Prince *et al.* 1998; Reynolds 2001; Batterbury *et al.* 2002; Prince 2002).

Prince (2002) strongly makes the case for quantitative assessment of land degradation through remote sensing. He argues that vegetation production which can be reliably measured from space is particularly useful since low productivity is at the heart of many land degradation definitions. In this dissertation remotely sensed data

were used to develop indicators of land degradation that can detect long-term reductions in vegetation production that cannot be explained by climate variability. Areas identified as degraded were compared to data on land use pressures to identify the human factors that might have caused degradation.

The human population of the Sahel is rapidly increasing (UN 2011). Pressure on the land is likely to increase accordingly (Barbier 2000; Reardon *et al.* 2001) and perhaps the extent and severity of land degradation. There is a pressing need for an objective and spatially explicit measure of land degradation and for an assessment of its linkages, if any, to human uses of the land (Batterbury *et al.* 2002; Dregne 2002; Safriel 2007b). The tragic shortage of data on human-induced land degradation is believed to have contributed to the failure of most interventions to reverse degradation and has brought about a policy dilemma on how to minimize further deterioration (Batterbury *et al.* 2002; Mortimore & Harris 2005).

## 1.2 Study area

Vjg"vgt o "ōUcjgnö"ku"qhvgp"cr rnkqf"vq"vjg" igpgtcn" tgi kqp"gzvgp fki" cetqu" the east-west extent of Africa and between the latitudes of roughly 10°N and 18°N (figure 1.1). The region includes the Sahelian, Sudano-Sahelian, Sudanian and parts of the Guinean eco-climatic zones (White 1983) and is characterized by a steep north-south gradient in mean annual rainfall (Le Houérou 1980b). Vegetation cover in the northern Sahel consists of shrubs interspersed between annual and perennial grasses, and further south by grasslands and deciduous, open savanna woodlands, with woody cover only locally exceeding 5%. The Sudanian zone is dominated by deciduous shrublands with sparse trees, and further south by deciduous woodlands with grass

understory. Finally, the Guinean zone is dominated by semi-deciduous closed woodlands and evergreen forests (Le Houérou 1980b; White 1983).

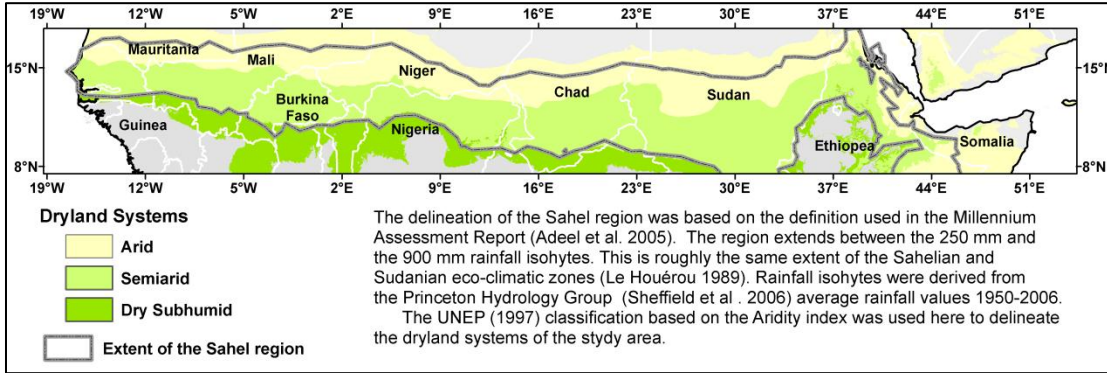


Figure 1.1 Dryland systems of the study area and the extent of the Sahel region.

Most of the Sahelian rainfall occurs during the northern hemisphere summer and is linked to periodic northwards excursions of the West African monsoon (Lebel *et al.* 2003; Dieng *et al.* 2008; Nicholson 2013). The onset of the monsoon proceeds slowly and is characterized by a succession of active and inactive phases (Lebel *et al.* 2003; Dieng *et al.* 2008). The initial wet spell in the northern Sahel does not usually produce significant rains. It is only when the Intertropical Convergence Zone (ITCZ) reaches the Sahelian ecoclimatic zone (Sultan & Janicot 2000b; Lebel *et al.* 2003; Sultan & Janicot 2003). The mean onset date of the wet season in the Sahelian zone is the 24<sup>th</sup> of June with a standard deviation of 8 to 10 days (Sultan & Janicot 2000a; Sultan & Janicot 2003; Dalu *et al.* 2009) and most rains fall between mid-July and September (Lebel *et al.* 2003). On average, the length of the wet season increases from about 50 days in northern Sahel at 18°N to about 100 days at 10°N (Zhang *et al.* 2005). Compared to the onset phase, the withdrawal phase is



relatively abrupt and rather uniformly distributed throughout the entire monsoon region (Nicholson 2013). The vegetation cycle closely responds to the seasonality in rainfall, with virtually all biomass production taking place in the wet summer months (Tucker *et al.* 1991; Tucker & Nicholson 1999; Herrmann *et al.* 2005a; Zhang *et al.* 2005).

During the last few decades, two sequences of extremely dry years in 1972-1973 and again in 1983-1984 struck the Sahel and were part of a longer drought that lasted from the end of the 1960s to the mid-1990s (Nicholson 2001; Le Barbé *et al.* 2002) (figure 1.2). This unusual dry spell was not limited to the Sahel but extended to regions more to the south as well (Le Barbé *et al.* 2002). The total number of rainfall events during the drought also decreased thus increasing the probability of dry spells during the rainy season (Le Barbé *et al.* 2002). Since 1994, annual rainfall totals somewhat recovered and varied around the mean of the standard climatological period of 1931-1960 (Nicholson 2001; Hiernaux *et al.* 2009b). These fluctuations in rainfall at intra-annual, interannual and decadal time scales made the Sahelian region of Africa the most dramatic example of climate variation that has been directly measured (Hulme 2001). The Sahel therefore provides (1) a valuable natural experiment on the effects of climatic variations on vegetation production and (2) a testing bed of indicators that attempt to differentiate climate-induced short-term ecosystem dynamics from land degradation.

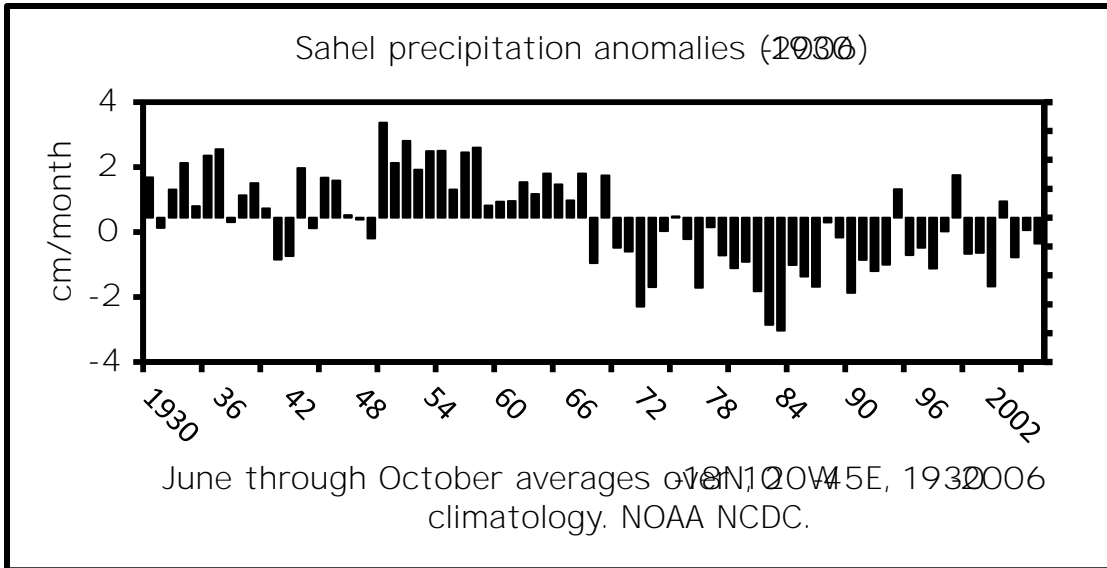


Figure 1.2 Wet season (June through October) Sahel precipitation anomalies (1930-2006). Data are from the National Oceanic and Atmospheric Administration (NOAA) National Climatic Data Center (NCDC).

### 1.3 The controversy surrounding land degradation in the Sahel

The Sahel region of Africa is sw rqugf"vq"dg"qpg"qh"vjg"y qtnfou" o quv"chhgevfg" areas by degradation (Oldeman *et al.* 1990; Le Houérou 1992; UNEP 1992). During the last few decades, high population growth rates in the Sahelian and Sudanian geqenk o cvke" |ppgu"\*eqmgevknxgn{" tghgttgf"vq" jgtg"cu"vjg"õUcjgnö."hkiwtg"3+ jcxg"dgpp" accompanied with cropland expansion and with an increase in livestock numbers (Vierich & Stoop 1990; Ramaswamy & Sanders 1992; van de Koppel *et al.* 1997; Lambin *et al.* 2003; FAO 2011). These changes in the Sudano-Sahelian agricultural and pastoral regions coincided with the Sahelian drought (late-1960s to the mid-1990s) (Nicholson 2001; Le Barbé *et al.* 2002). Commensurate with these changes in land use and with the drought were catastrophic reductions in crop yields and rangeland carrying capacity (Nicholson 1978; Lamb 1983; Hiernaux *et al.* 2009b).

The resulting famines of the 1970s and 1980s plus anecdotal accounts of progressive southwards march of the Sahara desert (Norman 1987; Lamprey 1988) led to the widely accepted narrative that population growth drives cropland expansion, overgrazing and infrastructure extension and that these changes in land use have resulted in widespread land degradation (e.g. Le Houérou 1996; Le Houérou 2002). Furthermore, Charney (1975) controversially suggested that overgrazing and land degradation may have even been the cause of the extreme droughts of the 1970s through positive feedback between rainfall and surface albedo. Faced with what has seemed at the time as a new and sinister problem threatening human well-being, the United Nations agencies initiated programs to combat land degradation despite the lack of substantiated information on its location, severity and causes (Prince 2002).

Following the 1974 drought, various attempts have been made to inventory land degradation and to provide a baseline for monitoring (Dregne 1977; Dregne 1983; Oldeman *et al.* 1990; Dregne & Chou 1992; Lepers 2003). Yet, the paucity of data on land degradation and the lack of any readily measured, objective indicators have inhibited progress (Prince 2002). Estimates of the extent of land degradation have ranged between 4% and 60% of the total area of the Sahel. Nevertheless, the figure of 60% degradation drawn from the Global Assessment of Soil Degradation (GLASOD; Oldeman *et al.* 1990) has been cited more often than the others (Safriel 2007a). The GLASOD study drew its estimates from judgment by regional soil experts. While subjective in its approach, it was based on more rigorous and consistent set of guidelines than previous assessments (Prince 2002). In addition to mapping the extent and severity of soil degradation, the GLASOD study included an

assessment of the human activities responsible for degradation. Its findings reinforced the preconceived narrative that overgrazing, cropland expansion and excessive fuel wood collection have caused widespread degradation.

Agronomists, geographers and development economists have tried to explain the findings of widespread degradation. Vierich and Stoop (1990) argued that drought reduced agricultural yields while rapid population growth increased demand for food. The widening gap between food supply and demand drove the vast majority of farmers to shorten fallow periods and to expand cultivation onto marginal lands thus increasing the risks of soil fertility depletion, erosion and crusting (Vierich & Stoop 1990; Vlek 1990; Swift *et al.* 1994; Bationo *et al.* 1998; Drechsel *et al.* 2001). Reardon *et al.* (2001) contended that capital deficiencies, the elimination of fertilizer subsidies, and poor accessibility to markets hampered the adjustments of farming practices that are necessary to counteract the threat of degradation. Reardon *et al.* (2001) view paralleled that of other economists (e.g. Breman 1997; Barbier 2000) and geographers (e.g. Webber 1996; Drechsel *et al.* 2001) who further argued that once degraded, agricultural lands were often abandoned and new lands were brought into production resulting in a perpetuating cycle of agricultural extensification and land degradation. Agricultural extensification is also believed to have contributed, at least in part, to rangeland degradation (van Keulen & Breman 1990; van de Koppel *et al.* 1997; Barbier 2000). In the Sahel, it was hypothesized that arable lands expanded at the expense of pastures consequentially increasing livestock densities in areas remaining accessible to pastoralists. In these rangelands, over-stocking is thought to have

perturbed vegetation cover sufficiently to expose soils to wind and water erosion as well as to crusting and compaction by animal trampling (Le Houérou 1980a; Olsson & Rapp 1991; Le Houérou 1996).

The evidence supporting many of the aforementioned arguments is, however, surprisingly slim (Turner *et al.* 1993). On one hand, the thesis that Sahelian agriculture tends to be mainly extensive and degrading has been found to be in discordance with crop yield data recorded between the 1960s and late 1990s (Hellden 1991; Breman 1998; Harris 1998; Niemeijer & Mazzucato 2002; Mortimore & Harris 2005). On the other hand, claims of widespread rangeland degradation through overgrazing run counter to long term increases in livestock populations (Sullivan & Rohde 2002; Mortimore & Turner 2005). Extensive studies in the Sudan (Olsson 1985; Ahlcrona 1988; Helldén 1991) have also demonstrated that earlier reports of serious human-induced land degradation (e.g. Hammer-Digernes 1977; Baumer & Tahara 1979) were rather misinterpretations of natural ecological adjustments to climatic fluctuations. They demonstrated that while droughts have reduced vegetation cover and agricultural yields, the return of more favorable climatic conditions has been accompanied with full recovery of land productivity, suggesting that there has been no degradation. Similarly, analysis of satellite data from 1982-onwards has revealed a consistent trend of vegetation recovery from the extreme droughts of the 1970s and early 1980s (Tucker & Nicholson 1999; Eklundh & Olsson 2003; Herrmann *et al.* 2005a; Olsson *et al.* 2005; Heumann *et al.* 2007a; Fensholt & Rasmussen 2011), suggesting that the perceived widespread degradation in the Sahel can be largely attributed to climate variability and not to irreversible

changes in land productivity (Prince *et al.* 1998; Herrmann *et al.* 2005a; Fensholt & Rasmussen 2011). Furthermore, interannual variations in agricultural yields per unit cultivated area in Burkina Faso and Nigeria; two countries identified by the GLASOD study as the most degraded in the Sahel; have been found to be strongly related to rainfall variability (Niemeijer & Mazzucato 2002). In fact, in these countries agricultural yields per unit rainfall have increased since the mid-1960s (Niemeijer & Mazzucato 2002; Mortimore & Harris 2005) raising the possibility that the extent and magnitude of adverse changes in soil properties reported by regional studies (Oldeman *et al.* 1990; Stoorvogel & Smaling 1990; Some *et al.* 1992) have been grossly overestimated (Niemeijer & Mazzucato 2002).

Other accepted tenets of human-induced land degradation have also been challenged. Studies in the Western Sahel have shown that the capability or willingness of farmers to invest in sustainable farming methods have been underestimated (de Ridder *et al.* 2004) and that the expansion of agriculture onto marginal lands did not necessarily result in degradation mainly due to investments in soil and water conservation measures and to the emergence of mixed livestock-farming systems (e.g. Tiffen *et al.* 1994; Adams & Mortimore 1997; Mazzucato & Niemeijer 2000; Mortimore & Harris 2005; Mortimore & Turner 2005).

None of these studies however claim that land degradation has not occurred in the Sahel. There are several well documented cases of local degradation resulting from the excessive utilization of the land with respect to its resilience (Geist & Lambin 2004) but the premise that regional degradation can be characterized using extrapolations from limited local scale data (e.g. Somé *et al.* 1992; Stoorvogel &

Smaling 1990; Le Houérou 1996) or d{"wruecnkpi"qh"nqecn"ögzrgtvö"qrkpkqpu"\*g0i0" Oldeman *et al.* 1990) are unwarranted and lack a certain objective rigor (Thomas & Middleton 1994; Prince *et al.* 1998; Stocking 2001; Batterbury *et al.* 2002; Koning & Smaling 2005; Mortimore & Turner 2005).

Several measurable indicators have been proposed to monitor land degradation such as: accelerated soil erosion rates (Stroosnijder 2007); deteriorating soil fertility (Batterbury *et al.* 2002); and long-term and irreversible reductions in vegetation cover or production efficiency (Nicholson *et al.* 1998; Prince *et al.* 1998; Batterbury *et al.* 2002; Prince 2002). However, soil measurements in the Sahel remain few and far between (Niemeijer & Mazzucato 2002; Fleitmann *et al.* 2007). Alternatively, long term and spatially contiguous changes in vegetation cover and its production, which are inherently linked to the major processes that lead to degradation (Prince 2002; Safriel 2007a; Nicholson 2011a), can be monitored using repeated satellite observations (e.g. Prince & Goward 1995; Myneni *et al.* 2002; Hansen *et al.* 2003; Running *et al.* 2004) and maybe able to answer some of the questions raised above.

#### **1.4 Temporal scales for the detection of land degradation**

It is generally agreed that human-induced land degradation is a long term process set in motion by inappropriate intensity or type of land use (Prince 2002; Wessels *et al.* 2007; Nicholson 2011a). Land uses which disturb vegetation cover and function may lead to the deterioration of the edaphic factors that contribute to plant growth (Schlesinger *et al.* 1990; Le Houérou 1992; Le Houérou 2002; Prince 2002). If so, the vegetation may transition to a new and less-productive vegetation

domain (Jeltsch *et al.* 1997; Prince 2002). As the degradation process proceeds, several transition domains may exist resulting in progressive and long term reductions in production efficiency (Jeltsch *et al.* 1997; Prince 2002; Nicholson 2011a); a concept that is embodied is state-and-transition models (Briske *et al.* 2005). The occurrence and severity of land degradation depend on the intensity of disturbances and the intrinsic characteristics of the soil, meteorological conditions, topography and post-disturbance land management (Lal *et al.* 1997; Eswaran *et al.* 2001). However, if land use intensity is reduced and vegetation recovers then there has been no degradation in the sense used here (Prince 2002). The time scale of post-disturbance vegetation recovery in the absence of soil degradation varies between biomes but field observations (Valone *et al.* 2002; Valone & Sauter 2005) and modeling studies (Wiegand & Milton 1996; Jeltsch *et al.* 1997; Weber *et al.* 2000) suggest time scales greater than 20 years. Therefore the time scales of observation necessary for monitoring land degradation should be greater than the normal sequence of vegetation recovery and the sequence of cultural practices such as periodic fallow and stocking rate cycles (Prince 2002).

## **1.5 Remote sensing of vegetation production**

The Advanced Very High Resolution Radiometer (AVHRR/2 and /3) instruments carried on NOAA's Polar-orbiting Operational Environmental Satellites (POES) have been providing global daily measurements since 1981 (Robel *et al.* 2009). The Normalized Difference Vegetation Index (NDVI) calculated from the AVHRR red and NIR spectral bands have been found to have a strong linear relationship with the fraction of photosynthetic active radiation absorbed by



vegetation canopy ( $f_{PAR}$ ) (Monteith 1972; Fuchs *et al.* 1984; Goward & Dye 1987; Sellers 1987; Goward & Huemmrich 1992; Myneni & Williams 1994; Sellers *et al.* 1997; Fensholt *et al.* 2006) and with maximum (i.e. unstressed) canopy photosynthetic uptake (Schloss *et al.* 1999; Merbold *et al.* 2009). This relationship has been exploited in light use efficiency (LUE) models to estimate Net Primary Production (NPP). The models require, in addition to  $f_{PAR}$ , incident PAR and measurements of the principal environmental stress factors, such as soil moisture, temperature and humidity. This approach (Prince & Goward 1995) has been adopted using the Moderate Resolution Imaging Spectroradiometer (MODIS) data as an operational, global productivity monitoring system (Running *et al.* 2004).

However, in arid and semi-arid areas, growing season sums of NDVI \* PFXk+cnqpg."ykvjqwv"vjg"qvjgt"eqo rqpqpvu"qh"c"NWG"oqfgn"fgo cpdfgf"d{"vjgqt{." have been found to be strongly related to NPP (Prince 1991; Rasmussen 1998; Seaquist *et al.* 2003) and above ground biomass measurements (Prince & Astle 1986; Prince & Tucker 1986; Fensholt *et al.* 2006). The reason for this is that the environmental stressors (e.g. acute water stress, intra-seasonal drought, land degradation) that limit photosynthetic canopy uptake generally induce changes in leaf display and hence in  $f_{PAR}$  and NDVI (Gamon *et al.* 1995; Wessels 2005). Similar to many earlier studies in drylands (e.g. Nicholson *et al.* 1990; Nicholson *et al.* 1998; Prince *et al.* 1998; Herrmann *et al.* 2005b; Olsson *et al.* 2005; Camberlin *et al.* 2007; Helldén & Tottrup 2008), growing season sums of NDVI will be used in this study as a proxy of vegetation productivity.

## 1.6 Monitoring land degradation with satellite remotely sensed data

A number of studies have demonstrated the utility of long term NDVI datasets to detect and monitor human-induced land degradation (e.g. Pickup & Chewings 1994; Geerken & Ilaiwi 2004; Li *et al.* 2004; Wessels *et al.* 2007). These studies have shown that in areas where vegetation production is tightly coupled to seasonal precipitation, human-induced land degradation results in negative temporal trends in vegetation production per unit rainfall. For example, Wessels *et al.* (2007) and Prince *et al.* (2009) found that in contrast to the non-degraded commercial areas, the excessively utilized and degraded communal areas in Zimbabwe and South Africa show a negative NDVI-rainfall relationship. Similar findings have been reported in the Syrian Steppe (Geerken & Ilaiwi 2004; Hirata *et al.* 2005), Australian drylands (Pickup & Chewings 1994) and in the Sahel (Herrmann *et al.* 2005). Nevertheless, precipitation is not the only factor that controls production and poor relations have been reported in the Sahel (Goward & Prince 1995a; Tracol *et al.* 2006; Williams *et al.* 2008; Hiernaux *et al.* 2009b; Hiernaux *et al.* 2009c; Fensholt & Rasmussen 2011) and elsewhere (Fuller & Prince 1996; Knapp & Smith 2001; Reynolds *et al.* 2004b). In areas where rainfall is not the only climatic factor limiting plant growth, negative temporal trends in vegetation production per unit rainfall do not necessarily indicate land degradation (Fensholt & Rasmussen 2011).

Several factors may influence the rainfall-production relationship in drylands. Nicholson *et al.* (1990), Fuller & Prince (1996) and Potts *et al.* (2006), for example, found positive feedbacks between vegetation production and antecedent rainfall at

monthly and interannual timescales. These feedbacks are sometimes likened to a  $\delta$  (Goward & Prince 1995b; Prince & Goward 2000; Wiegand *et al.* 2004) and can arise from purely physical reasons, such as soil moisture carried over from antecedent rainfall (Goward & Prince 1995a; Fuller & Prince 1996) or can result from inter-annual carryover of soil nutrients and seed banks (Lauenroth & Sala 1992; Nouvellon *et al.* 2001; Oesterheld *et al.* 2001). Such relations, however, are complex and feedbacks are not found in all climatic vegetation types (Fuller & Prince 1996; Grist *et al.* 1997). For instance, Reynolds *et al.* (2004a) and Knapp *et al.* (2008) argue that, in most ecosystems, growing-season precipitation should have the most direct impact on vegetation production. On one hand, a large portion of Sahelian precipitation falling at the beginning of the wet season may be lost to evaporation before it can be used for photosynthesis (Huxman *et al.* 2004) and, while early season precipitation event(s) may trigger germination of annual plants, seedling development and culm elongation are aborted unless subsequent rain events allow seedlings to survive and grow (Elberse & Breman 1989; Elberse & Breman 1990; Huxman *et al.* 2004; Hiernaux *et al.* 2009c). On the other hand, precipitation falling after fructification is not used for production by most annuals (Hiernaux *et al.* 2009c) and, while leaves of trees and some shrubs developed early in the growing season are usually retained until late in the season, they typically have lower photosynthetic capacity than younger leaves (Chabot & Hicks 1982).

The frequency and intensity of precipitation events can also influence vegetation production (Noy-Meir 1973; Sala & Lauenroth 1982; Prince *et al.* 1998; Wainwright *et al.* 1999; Jobbagy & Sala 2000; Paruelo *et al.* 2000; Knapp & Smith

2001; Knapp *et al.* 2002; Reynolds *et al.* 2004b; Schwinning & Sala 2004; Knapp *et al.* 2008; Williams *et al.* 2008; Heisler-White *et al.* 2009; Robertson *et al.* 2009) either by altering soil moisture levels (Lebel *et al.* 2003; Knapp *et al.* 2008; Good & Caylor 2011) or nutrient availability (Belnap *et al.* 2005) or both. A number of field experiments in North American grasslands and shrublands have demonstrated the sensitivity of vegetation production to an intensified precipitation regime (Jobbagy & Sala 2000; Paruelo *et al.* 2000; Knapp & Smith 2001; Knapp *et al.* 2002; Heisler-White *et al.* 2009; Robertson *et al.* 2009). For the same amount of total rainfall, vegetation production in dry biomes have been found to respond positively to more intense and less frequent precipitation events, whereas in the wetter biomes vegetation production have been found to decrease in response to an intensified precipitation regime (Knapp & Smith 2001; Knapp *et al.* 2002; Heisler-White *et al.* 2009). Modeling studies suggest that this asymmetrical response to precipitation regimes is mainly due to differences between biomes in the proportional losses of precipitation to evaporation and runoff (Reynolds *et al.* 2004b; Knapp *et al.* 2008).

In addition to the timing, frequency and intensity of precipitation events, air humidity and temperature can also affect vegetation production either directly by influencing stomatal conductance and photosynthetic reaction rates (Collatz *et al.* 1991; Collatz *et al.* 1992; Reichstein *et al.* 2007; Williams *et al.* 2008) or indirectly by altering soil evaporative demands (Xue *et al.* 1991a; Reichstein *et al.* 2007). By analyzing eddy-covariance measurements across a range of vegetation types and climate zones in Africa, Merbold *et al.* (2009) found strong relations between net photosynthetic accumulation by C<sub>3</sub>-plants and vapor pressure deficit but these

relations were poor to non-existent at the C<sub>4</sub>-plant dominated sites. These and land surface modeling studies that have investigated the relative influence of climatic factors on vegetation production have indicated that in addition to precipitation, air humidity (Williams *et al.* 2008) and temperature (Beer *et al.* 2010) may play an important, yet secondary role in limiting vegetation production in drylands.

Similar to many earlier studies (e.g. Goward & Prince 1995a; Tracol *et al.* 2006; Williams *et al.* 2008; Hiernaux *et al.* 2009b; Hiernaux *et al.* 2009c), Fensholt & Rasmussen (2011) found that the inter-annual variations in vegetation production were poorly explained by annual rainfall totals. It is very likely that in addition to precipitation, other climate factors acted synergistically to influence vegetation production by altering soil moisture levels (Sala *et al.* 1988; Epstein *et al.* 1997; Lebel *et al.* 2003; Reichstein *et al.* 2007; Knapp *et al.* 2008; Good & Caylor 2011), nutrient levels (Belnap *et al.* 2005), and stomatal resistance and photosynthetic reaction rates (Collatz *et al.* 1991; Collatz *et al.* 1992; Williams *et al.* 2008; Merbold *et al.* 2009; Beer *et al.* 2010). This suggests that it might be necessary to account for climate factors other than precipitation alone in order to distinguish between climate-induced fluctuations in vegetation production and human-induced changes which are generally more subtle and gradual (Evans & Geerken 2004; Fensholt & Rasmussen 2011).

It is unlikely that any stand-alone remote sensing-based method will be able to unequivocally map human-induced land degradation. In addition, the evaluation of these methods has proven difficult owing to the paucity of field validation data (Batterbury *et al.* 2002; Wessels *et al.* 2008). Also, remotely sensed indicators

provide little if any information on the social processes that give rise to degraded landscapes. To complement the monitoring process, Batterbury *et al.* (2002) and Nicholson (2011a) argue that it is important to identify the human factors that act as drivers to degradation not only to alert officials to unsustainable land use practices but also to determine whether long term reductions in production efficiency are in fact human-induced. Recent studies have produced highly resolved spatial data on human demographics and anthropogenic uses of the land (Imhoff *et al.* 2004; CIESIN 2005; Robinson *et al.* 2007; Ramankutty *et al.* 2008). These data, together with remotely sensed indicators of land degradation, can be used to investigate the spatial component of demographic and anthropogenic land use pressures.

## **1.7 Research Objectives**

The fundamental goal of this dissertation is to examine whether there is evidence of human-induced land degradation in the Sahel and, if so, its location and intensity. The general hypothesis was that long-term negative trends in production efficiency can be used to detect human-induced land degradation. To test whether the negative trends were in fact human-induced, they were compared with the available data on population density, land use and land biophysical properties that determine the susceptibility of land to degradation.

The following specific research objectives were addressed:

1. Characterize the correlations between remote sensing estimates of vegetation production and the meteorological variables, namely precipitation, seasonal precipitation distribution, air humidity and temperature. (Chapter 2)

2. Explore the biophysical mechanisms of vegetation response to climate variability at the process level using a Soil-Vegetation-Atmosphere Transfer (SVAT) model. (Chapter 2)

3. Identify any long term trends in vegetation production which are not caused by natural ecological adjustments to episodic droughts and changes in air humidity and temperature. (Chapter 3)

4. Explore the relationship between long-term trends in vegetation production, population density, human appropriation of NPP, livestock, and cropping. (Chapter 4)

## 1.8 Outline of Dissertation

This dissertation consists of five chapters. Chapter 1 introduces the topic of land degradation, reviews the ongoing debate on the extent, severity and causes of land degradation in the Sahel and sets the research objectives. In Chapter 2, the time series of precipitation and meteorological variables from 1982 to 2006 are characterized for the study area. This was done to identify the meteorological variables that influence vegetation production. The biophysical mechanisms that can explain the observed relationship are explored using a SVAT model.

Climate-vegetation relationships were used to estimate potential vegetation response of vegetation to climate variability alone excluding other factors that limit

vegetation production, including human land use. The residuals (observed  $\delta$  potential PFXK+) were used to normalize for the effects of climate variability on vegetation production (Prince 2002; Geerken & Ilaiwi 2004). Significant negative residual trends were then mapped to identify areas where there may be human-induced land degradation. This approach is similar to the method which was used to identify negative trends in the production-rainfall relationship in the degraded areas of South Africa and Syria (Prince 2002; Hirata *et al.* 2005; Wessels *et al.* 2007) but extends the climatic controls to include in addition to rainfall the other meteorological variables that were found to influence vegetation production. However, it should be stressed that even when NDVI or NPP falls below the potential set by the meteorological conditions, the cause is not necessarily human-induced.

Chapter 4 compares the residual trend maps with the available data on population density and land use to investigate whether the type and intensity of land use is associated with negative trends in vegetation production. Furthermore, chapter 4 investigates whether the influence of land use varies with the geography of land biogeophysical properties that determine the resilience of land to degradative processes. Chapter 5 summarizes the findings, discusses the limitations of remotely sensed estimates of land degradation, and how these limitations may be addressed in future research. Finally, the methods used for the reconstruction of daily AVHRR NDVI data are presented in Appendix I.



## 2.1 Introduction

The effect of climate variation on vegetation production is a major research focus in African drylands (Fuller & Prince 1996; Olsson *et al.* 2005; Hiernaux *et al.* 2009c) and elsewhere (Goward & Prince 1995a; Fang *et al.* 2001; Nemani *et al.* 2003). More recently, interest has intensified as global circulation models project an increase in inter-annual precipitation variation, higher temperatures, and an intensified precipitation regimes (through larger individual precipitation events) with longer intervening dry periods than at present (Easterling *et al.* 2000; IPCC 2007).

Vegetation production in drylands is often assumed to be closely related to inter-annual rainfall variability (Le Houérou *et al.* 1988; Herrmann *et al.* 2005a). Le Houérou (1984) suggested that the ratio of NPP to precipitation (Rain Use Efficiency, RUE) in drylands has a stable value (6.7). Wessels *et al.* (2007) and Nicholson *et al.* (1990) found moderate to strong linear relationships between rainfall and vegetation production in parts of arid and semi-arid South Africa and the Sahel. Nevertheless, precipitation is not the only factor that controls production and poor relations have been reported in the Sahel (Goward & Prince 1995a; Tracol *et al.* 2006; Williams *et al.* 2008; Hiernaux *et al.* 2009b; Hiernaux *et al.* 2009c; Fensholt & Rasmussen 2011) and elsewhere (Fuller & Prince 1996; Knapp & Smith 2001; Reynolds *et al.* 2004b).

In drylands, soil properties, the frequency and intensity of rainfall events, air humidity and temperature combine to influence vegetation production (Noy-Meir

1973; Prince *et al.* 1998; Sankaran *et al.* 2005; Williams *et al.* 2008; Good & Caylor 2011) by altering infiltration rates, evaporative demands, nutrient availability and leakage losses from the soil column (Sala *et al.* 1988; Epstein *et al.* 1997; Lebel *et al.* 2003; Reichstein *et al.* 2007; Knapp *et al.* 2008; Good & Caylor 2011). Furthermore, air humidity and temperature may also directly influence vegetation production by altering stomatal resistance and photosynthetic reaction rates (Collatz *et al.* 1991; Collatz *et al.* 1992; Williams *et al.* 2008; Merbold *et al.* 2009; Beer *et al.* 2010).

While several remote sensing studies have investigated the nature of the relation between NDVI (used as a proxy of vegetation productivity) and rainfall in the Sahel (e.g. Nicholson *et al.* 1990; Nicholson *et al.* 1998; Prince *et al.* 1998; Herrmann *et al.* 2005b; Olsson *et al.* 2005; Camberlin *et al.* 2007; Helldén & Tottrup 2008), only few studies have expanded beyond that to include other meteorological variables that might influence vegetation production (Nemani *et al.* 2003; Beer *et al.* 2010).

The purpose of this study was twofold; (i) to characterize empirically the nature of the relationship between remotely sensed estimates of vegetation production and climate variability and (ii) to explore, using a land surface model, the underlying hydraulic and biophysical processes to which these relationships can be attributed.

Bias-corrected-hybrid meteorological datasets constructed by combining a suite of global observation-based datasets with numerical weather prediction and assimilation models are becoming available at higher temporal and spatial resolutions (Sheffield *et al.* 2006). These, along with recent developments in Advanced Very

High Resolution Radiometer (AVHRR) data processing (Pedelty *et al.* 2007), provided the opportunity to expand on previous studies of vegetation responses to climate variability (Nicholson *et al.* 1990; Helldén 1991; Olsson & Rapp 1991; Nicholson 2001; Nemani *et al.* 2003; Herrmann *et al.* 2005a; Olsson *et al.* 2005; Helldén & Tottrup 2008; Hiernaux *et al.* 2009c; Beer *et al.* 2010).

While the empirically derived relationships may reveal the direction and magnitude of vegetation responses to climate variation, they offer little understanding of the underlying biophysical processes to which these relations can be attributed. To address this problem, a land surface model was used to explore these processes. The model selected was the Simplified Simple Biosphere (SSiB2 ver.2) (Xue *et al.* 1991b; Zhan *et al.* 2003). SSiB2 is a process-oriented model that simulates explicitly the interactions between climate, soil, and plants. In SSiB2, the rates of carbon sequestration change with temperature, the proportion of incident photosynthetically active radiation absorbed by green vegetation (fPAR), and intracellular CO<sub>2</sub> concentration. The Farquhar and Collatz (Farquhar *et al.* 1980; Collatz *et al.* 1991; Collatz *et al.* 1992) formulations are used to model CO<sub>2</sub> uptake within the leaf. CO<sub>2</sub> uptake at the canopy scale is regulated by stomatal conductance which, in turn, is limited by stress multipliers of air-to-leaf vapor pressure deficit and soil moisture (Zhan *et al.* 2003). The focus of the modeling approach was to investigate, in different climates and for different vegetation types, the sensitivity of soil moisture, leaf temperature, and stomatal conductance to changes in precipitation, temperature, and humidity and whether climate-induced changes in soil moisture, stomatal conductance and leaf temperature, if any, influence vegetation production.

Establishing the relationship between remotely sensed estimates of vegetation production and meteorological variables is essential for developing a reliable land degradation monitoring approach that is capable of distinguishing human-induced land degradation from climate-induced vegetation dynamics (Reynolds 2001; Prince 2002; Geerken & Ilaiwi 2004).

## **2.2 Material and Methods**

### **2.2.1 Remote sensing data**

Version 2 of the Long-term Data Record (LTDR) daily time series of the National Oceanic and Atmospheric Administration (NOAA) AVHRR Global Area Coverage (GAC) reflectance data (Pedelty *et al.* 2007) for the years 1982 to 2006 were used in this study (<http://ltdr.nascom.nasa.gov>). While the spatial resolution of the AVHRR instrument is ~1.1 km at nadir, the NOAA satellites transmit the reduced resolution (~4.4 km) GAC data generated onboard by averaging the reflected radiances from a sample of four out of every five measurements along every third scan line (i.e. a sampling frequency of 4 out of every 15 measurements) (Kidwell 1998). The LTDR data processing stream ingests the GAC data from NOAA satellites 7,9,11 and 14 and creates a daily reflectance product using a geographic projection at a spatial resolution of 0.05°. LTDR data processing includes a vicarious sensor calibration of the red (0.5860.68 µm) and near infrared (0.72561.10 µm) channels using cloud/ocean techniques to remove variations caused by changes in sensors and sensor drift (Vermote & Kaufman 1995; Vermote & Saleous 2006a). LTDR processing also includes an improved atmospheric correction scheme to reduce

the effects of Rayleigh scattering, ozone, and water vapor but does not include corrections for the effects of aerosols (Pedelty *et al.* 2007).

For the present study, the LTDR reflectances in the red (0.5860.68  $\mu\text{m}$ ) and near infrared (NIR) (0.72561.10  $\mu\text{m}$ ) were: (1) spatially aggregated to 0.15° (3x3 pixels); (2) normalized to a standard sun-target-sensor geometry; and (3) filtered for cloud-contaminated observations which were then replaced with reconstructed values interpolated from preceding and succeeding clear-sky observations. An account of the Bidirectional Reflectance Distribution Function (BRDF) correction, cloud filtering, and interpolation procedures is given in Appendix 1. Daily NDVI values were subsequently calculated ( $\text{NDVI} = (\text{NIR} - \text{red}) / (\text{NIR} + \text{red})$ ).

Spatial aggregation to 0.15° reduces most of the errors introduced by the GAC sampling scheme (Rembold & Maselli 2010) and aggregation to 0.25° or 0.35° only results in marginal further improvements (Nagol 2011). Because of this, analyses of the AVHRR data were conducted at 0.15° spatial resolution.

BRDF and atmospheric corrections reduce noise in surface NDVI data (Nagol *et al.* 2009) that would otherwise result from the strong bidirectional properties of vegetation (Gutman 1991; Vermote *et al.* 2009a; Fensholt *et al.* 2010) and the considerable absorption in the AVHRR NIR channel by atmospheric water vapor (Cihlar & Howarth 1994). The resulting daily data were intended to enable more precise identification of vegetation dynamics (Viovy *et al.* 1992) than maximum value compositing (generally 10 days or monthly), particularly in the drier areas with short growing season.

### 2.2.2 Meteorological data

The Princeton Hydrology Group (PHG) 1.0° dataset of daily precipitation, surface air temperature, specific humidity, atmospheric pressure and incident solar radiation (Sheffield *et al.* 2006) were used in this study. The dataset is constructed from the NCEP-NCAR<sup>2</sup> reanalysis data and corrected for biases using observation based datasets of precipitation and air temperature. Daily data for the period 1982-2006 were downscaled from 1° to the 0.15° resolution of the AVHRR dataset using bilinear interpolation.

### 2.2.3 Estimating phenological transition dates and the length of the growing season

The rates of change of daily NDVI data were used to define key phenological transition dates of the growing season (Zhang *et al.* 2003). Green-up, maturity, senescence and dormancy; respectively. Green-up is the date when NDVI begins to increase rapidly indicating the onset of leaf development. Maturity is the date when the rate of increase in NDVI slows and NDVI approaches its maximum indicating peak green leaf area. Senescence is the date when NDVI begins to decrease rapidly indicating leaf senescence. Dormancy is the date when NDVI approaches its minimum annual value owing to death of annuals and suspension of growth and true dormancy in perennials.

---

<sup>2</sup> NCEP-NCAR: National Center for Environmental Prediction(NCEP) & National Center for Atmospheric Research(NCAR)

To estimate the phenological transition dates, piecewise sigmoid functions (equation 2.1) were fitted to periods of sustained NDVI increase (i.e. growth) and decrease (i.e. senescence). The rates of change in the curvature of the fitted sigmoid functions (i.e. the second derivative) were then calculated. During the period of sustained NDVI increase, the local maxima of the second derivative were used for the dates of green-up and maturity, and the local minima of the second derivative during the period of sustained NDVI decrease were used for senescence and dormancy (Zhang *et al.* 2003). The phenological transition dates were compared with MODIS Land Cover Dynamics Science Dataset Collection 4 (Zhang *et al.* 2006) during the overlapping period (2002-2006).

---

where  $t$  is time in days,  $y(t)$  is the NDVI value at time  $t$ ,  $a$  and  $b$  are fitting parameters,  $d$  is the initial minimum NDVI value and  $c+d$  is the maximum NDVI value.

The onset of leaf development and leaf senescence were then used to define the timing and duration of the growing season. Annual and growing season sums of daily NDVI, precipitation, temperature, and humidity were calculated for each year (1982-2006).

**4 0 4 0 6 " T g n c v k q p u j k r " q h " c precipitation' P F X K " y k v j " c p**

The relationships of annual and growing season sums of precipitation and PFXK were characterized using linear regressions for every three by three pixels. The coefficients of determination ( $r^2$ ) were mapped to show the geographical patterns

of the PFXK -total precipitation relationships for the entire year and for the growing season alone.

#### **4 0 4 0 7 " T g n c v k q p u j k r " q h " i t q y k p i " u g c u q p " P F X K distribution**

A series of small precipitation events may have a different effect on vegetation production than an equivalent amount of rainfall occurring in a few intense events (Reynolds *et al.* 2004b; Good & Caylor 2011). To describe the statistical manner by which precipitation arrived on the landscape, two higher order moments of intraseasonal precipitation distribution were calculated from daily precipitation data. These were the growing season precipitation variance and its skewness. Summary statistics were used since it is impractical to specify explicitly the enormous number of seasonal patterns of rainfall frequency and amount that can occur for more than a few pixels. High precipitation distribution variance indicates higher than normal deviation from mean seasonal precipitation and can result from extended periods of drought or from intense precipitation events or a combination of both, while the skewness is a measure of the dominant frequency of either high intensity precipitation events (negative skewness) or low intensity precipitation events (positive skewness).

Vjg" tgnckqp" qh" itqyki" ugcup" PFXK" vq" ugcupcn" rtgekrkvcvkqp" vqvcnu." precipitation variance and skewness were characterized using multivariate linear regression analysis. To reduce the effects of multicollinearity between input variables and consequent overfitting (Dielman 2005), a subset of independent variables that ÷dguvø" gzrnckpgf" PFXK" xctkckqp" ygtg" ugngevgf" hqt" gcej" 5" d{ " 5" rkzgnu" wukpi" vjg" computational approach of (Furnival & Wilson 1974).



The computational approach of (Furnival & Wilson 1974) searches for the variable subsets with the highest  $r^2$  value adjusted for degrees of freedom (adjusted  $r^2$ ). The variables of the regression model with the highest adjusted  $r^2$  were tested for multicollinearity and the model regression coefficients were tested to determine whether they were significantly different from zero. To test for multicollinearity, the variance inflation factors (VIFs) of the model independent variables were evaluated relative to the  $r^2$  value of the model (Dielman 2005a). Multicollinearity was considered strong enough to affect the model coefficient estimates whenever any of the VIFs was larger than  $1/(1-r^2)$  (Freund & Wilson 1998). A t-test was used to test the null hypothesis that the model regression coefficients  $B_{m-1}$  were equal to zero. If there was insufficient evidence to reject the null hypothesis ( $H_{0:m-1} : \beta_{m-1} = 0, p > 0.05$ ) or if multicollinearity was strong enough to affect model estimates then the regression model with the second to highest adjusted  $r^2$  was subjected to the same tests. The procedure was repeated until the test conditions were met.

#### **4.0.4.0.8 "T g n c v k q p u j k r " q h " i t q y k p i " u g c u q p " P F X K distribution**

Vjg"tgnckqpukru"qh"itqykpi"ugcuqp" PFXK"cpf"ugcuqpcn"rtgekrkvcvkqp"vqvcnu." specific humidity and air temperature were characterized by regression analysis using the same computational approach described in the previous section. Furthermore, the vjtg"ogvgtqngqikecn"xctkcdngu"cpf"vjg" PFXK"fcvc"ygtg"uvcpfctfk|gf"vq" |gtq"ogcp" and a standard deviation of one. The standardized regression coefficients were then estimated to measure the relative contribution of each meteorological variable to the qdugtvgf" PFXK" xctkcvkqp0" " Vjg" uvcpfctfk|gf" tgitguukqp" eqghhkekpvu" ygtg"" summarized by the landcover types in the study area (Friedl *et al.* 2002) in order to

characterize the relative contribution of each of the meteorological variables to the observed NDVI variation in grasslands, shrublands, and savannas.

## **2.2.6 Soil-vegetation-atmosphere transfer modeling**

### *2.2.6.1 Model description*

The Simplified Simple Biosphere (SSiB2 ver.2) land surface model (Xue *et al.* 1991b; Zhan *et al.* 2003) represents plant canopy structure and plant physiology as driven by prescribed meteorology and vegetation phenology. SSiB2 is a simplified version of the Simple Biosphere model (SiB) originally designed by (Sellers *et al.* 1986). SSiB2 models vegetation as a single layer instead of the two in SiB, and implements a less computationally expensive scheme to calculate aerodynamic resistance. In addition, the prognostic equations in SiB that relate stomatal conductance to soil moisture and calculate the diurnal variation in radiation absorption and albedo are replaced with empirical relations that require fewer parameters. SSiB2 replaces Jarvis (1976) with a modified version of Farquhar *et al.* (1980) biochemical photosynthesis model (Collatz *et al.* 1991; Collatz *et al.* 1992), scaled by the canopy integration scheme of (Zhan *et al.* 2003) and coupled to the Ball-Berry semi-empirical stomatal conductance model so that stomatal conductance and canopy net photosynthesis are estimated simultaneously. In the model, the rate of photosynthesis changes with temperature,  $f_{PAR}$ , and intercellular CO<sub>2</sub> concentration. The latter is regulated by stomatal conductance. Stomatal conductance is limited by stress multipliers of air-to-leaf vapor pressure deficit and soil moisture (Zhan *et al.* 2003). The SSiB2 standard model parameters have been refined for several soils and vegetation functional types (Chen *et al.* 1996; Xue *et al.* 1996a; Xue *et al.* 1996b;

Schlosser *et al.* 1997; Zhan *et al.* 2003; Sun & Xue 2004), including some of those found in the Sahel region (Kahan *et al.* 2006).

Parameterization and validation studies and land surface model inter-comparison experiments (Robock *et al.* 1995; Wetzel *et al.* 1996; Liang *et al.* 1998; Lohmann *et al.* 1998; Wood *et al.* 1998) have demonstrated that SSiB2 can reasonably reproduce measured energy and water fluxes at diurnal, seasonal, and multi-annual scales across diverse climates and vegetation functional types.

#### 2.2.6.2 Sensitivity experiments

SSiB2 was used to explore the underlying hydrological and physiological processes to which the empirical relationships, revealed in the statistical analysis of co-variation between meteorology and vegetation productivity, can be attributed. The model was run for the period 1999-2007 with a 3-hourly time step for a number of sites representative of different vegetation types and climatologies throughout the Sahel (table 2.1). Model inputs for the base run were Princeton Hydrology Group meteorology, LAI and fraction vegetation cover (Baret *et al.* 2007).

To investigate the sensitivity of vegetation to precipitation variation during the early stages of phenological development (i.e. greenup to maturity), SSiB2 was run eight times with the precipitation data modified for the corresponding period ( $\pm 0.5$ ,  $\pm 1$ ,  $\pm 1.75$  and  $\pm 2.5$  standard deviations from the values used in the base run; changed values that exceeded the range of long term (1982-2007) natural meteorological variation were reset to the minimum and maximum of observed meteorological variation, as appropriate) while keeping the remaining meteorological variables

unchanged. The sensitivity experiments were repeated for the maturity stage (i.e. from maturity to senescence). The same approach was used to investigate the sensitivity of vegetation to changes in humidity and temperature. The resulting changes in soil moisture and stomatal conductance and their relation to canopy scale net photosynthesis were summarized at a daily time step and averaged over each of the two stages of phenological development.



## 2.3 Results

### 2.3.1 Phenological transition dates

For the transition dates of greenup, maturity and senescence, the comparison between the AVHRR and MODIS (Zhang *et al.* 2006) measurements revealed a good agreement with root mean square errors only slightly higher than the reported accuracies of the MODIS products (Zhang *et al.* 2003; Zhang *et al.* 2006). However, the measurements of the dormancy transition dates did not agree and the root mean square error (RMSE = 29 days) of the dormancy comparison was one order of magnitude higher than the RMSE values for greenup, maturity and senescence (figure 2.1). This is perhaps due to the less pronounced transitions in the rates of change in NDVI curvature towards the end of the growing season which renders derivatives of the dormancy dates more sensitive to errors in NDVI measurements.

The greenup transition dates were characterized by a pronounced north-south gradient but with the dates detected earlier at higher latitudes (late August) than at lower latitudes (late October). Both dates were found to vary between years with grasslands in the arid region showing the highest temporal variability in greenup dates. On average, the length of the growing season (the difference between the two dates) varied from approximately 20 days at the southern edge of the Sahara desert to approximately 250 days in the wetter parts of the study area (figure 2.2).

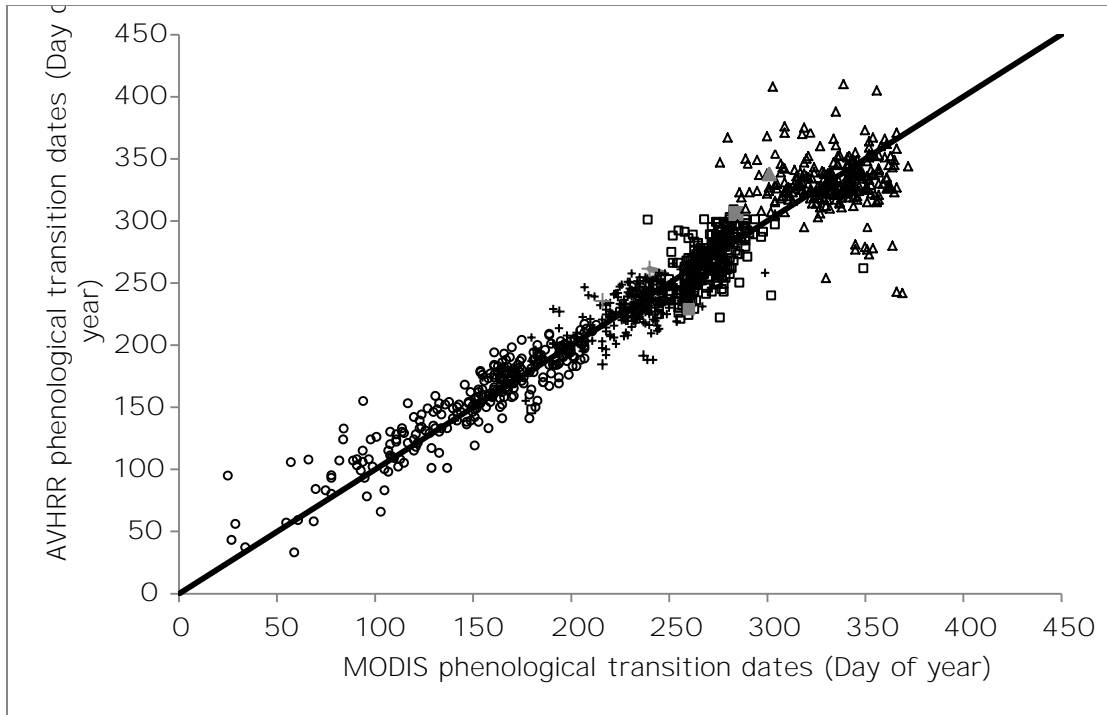


Figure 2.1 Scatter plot of MODIS and AVHRR phenological transition dates of 250  
 onset of greenness increase (RMSE = 15.5 days,  $r=0.89$ ). Crosses (+) represent the  
 dates of onset of greenness decrease (RMSE = 17 days,  $r = 0.63$ ). Open triangles  
 represent the dates of onset of greenness decrease (RMSE = 17 days,  $r = 0.63$ ).

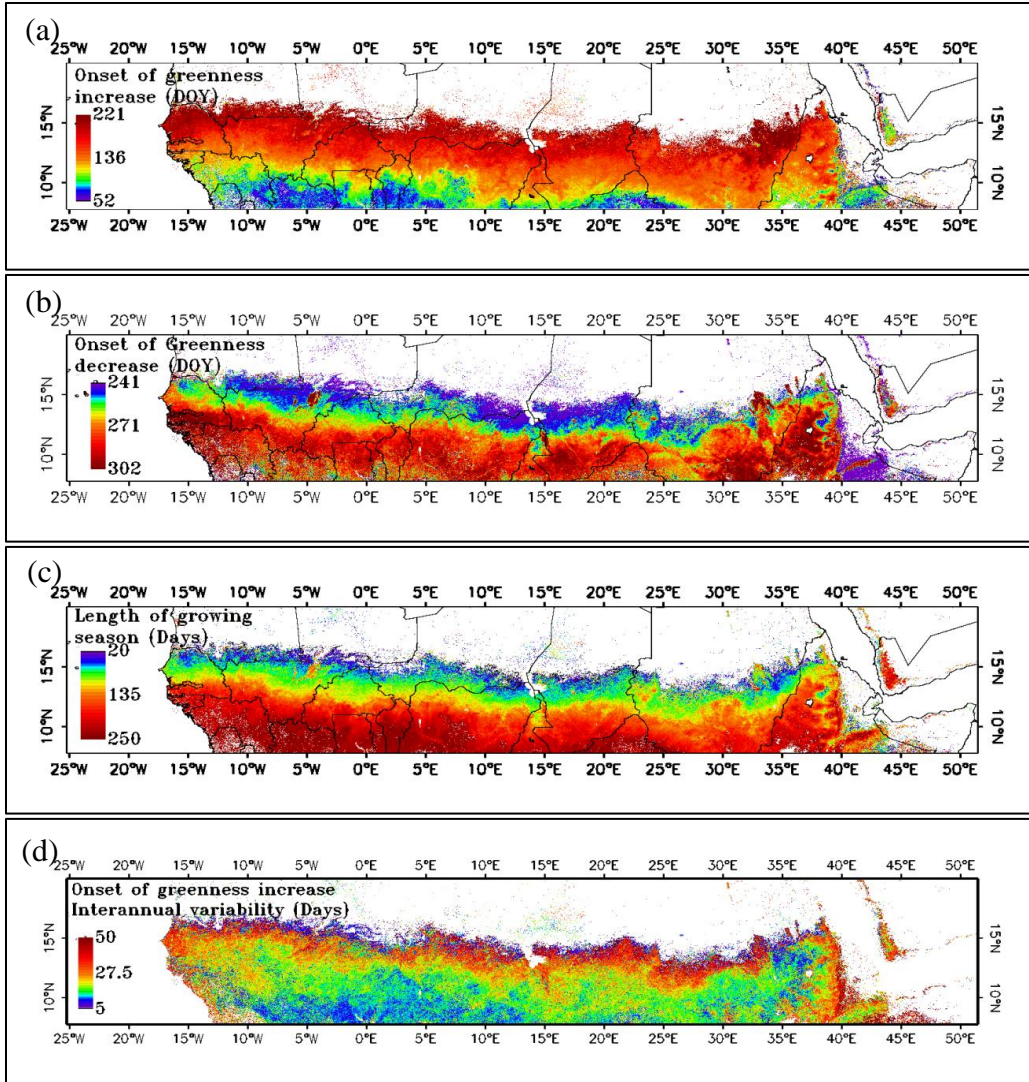


Figure 2.2 Spatial variation in averaged values (1982-4228+) of the onset of greenness increase (DOY), the onset of greenness decrease (DOY), the length of growing season (days). The map in (d) is the between years variation ( $\pm 2$  standard deviations) in the onset date of greenness increase. The abbreviation DOY is the Julian day of the year.

### 2.3.2 Relationship of NDVI with rainfall

The relationships of annual and growing season sums of rainfall and NDVI differed in strength and to some extent in their spatial patterns. The growing season rainfall- PFXK" tgnckpqujkru" ygtg" igpgtcm{" vjg" uvtqpig" qpg" \*hkiwtg" 405+0" Vjg"



growing season rainfall- PFXK<sup>3</sup> in approximately 58% of the study area whereas the annual rainfall- PFXK relationships were significant in 37% of the study area.

C"dgnv"qh"uki pkhkecpv"cppwcn" PFXK-rainfall relationships was evident around the 700mm rainfall isohyet (figure 2.3a). However, areas receiving less than 400mm rainfall/year and areas receiving more than 1000mm rainfall/year were generally characterized by insignificant relationships (figure 2.4). On average, stronger itqykp<sup>4</sup> PFXK-rainfall relationships were found in the arid and semi-arid areas with shrubland and grassland landcover ( $r^2 = 0.43 \pm 0.17^4$ ) than in sub-humid areas with woody savanna land cover ( $r^2 = 0.3 \pm 16^4$ ).



Figure 2.3 Coefficients of determination ( $r^2$ ) for (a) annual rainfall- PFXK<sup>3</sup> and growing season rainfall- PFXK<sup>3</sup> relationships for the 300mm, 700mm and 1100mm rainfall isohyet.

<sup>3</sup> Critical t-values calculated for each pixel indicated that, in general, regressions with  $r^2$  values greater than 0.3 were significant ( $p < 0.05$ ).

<sup>4</sup> Mean  $\pm$  one standard deviation











































































































































































































































































































